

## THE IMPACT OF ENERGY-FILTERING TRANSMISSION ELECTRON MICROSCOPY FOR THE STUDY OF CORROSION AND FILMING BEHAVIOUR OF ALUMINIUM ALLOYS

K.Shimizu, G.M.Brown\*, H.Habazaki\*\*, K.Kobayashi\*, P.Skeldon\*\*\*, G.E.Thompson\*\*\*, and G.C.Wood\*\*\*

University Chemical Laboratory, Keio University 4-1-1 Hiyoshi, Yokohama 223, Japan,

\*Department of Chemiatry, Faculty of Science and Technology, Keio University, 3-14-1 Hiyoshi, Yokohama 223, Japan,

\*\*Institute for Materials Research, Tohoku University, Katahira, Sendai 980-77, Japan,

\*\*\*Corrosion and Protection Centre, UMIST, Manchester M60 1QD, U.K.

**ABSTRACT** Through the study of the growth of porous anodic films on an Al - 1.4 wt% Fe alloy containing finely dispersed  $\text{Al}_6\text{Fe}$  and  $\text{Al}_3\text{Fe}$  particles, the enormous potential of the combined use of ultramicrotomy and energy-filtering transmission electron microscopy in the studies of this kind is demonstrated. The approach is particularly powerful and important in situations where the aluminium surfaces are microscopically heterogeneous, such as many aluminium alloys of practical importance. Thus, morphologies, structures, and elemental distribution maps of local regions of interest, associated with the presence of finely dispersed  $\text{Al}_6\text{Fe}$  or  $\text{Al}_3\text{Fe}$  particles, have been clarified with great precision. Additionally and importantly, complex interfacial processes associated with the growth of anodic oxide on these intermetallic particles which, for the  $\text{Al}_6\text{Fe}$  case, leads to the initial, selective oxidation of aluminium and consequent enrichment of iron in the  $\text{Al}_6\text{Fe}$  phase immediately beneath the oxide, have been revealed for the first time.

**Keywords:** *aluminium alloy, second phase, anodic oxidation, EELS imaging*

### 1. INTRODUCTION

Porous anodic film formation over aluminium alloys of practical importance is considerably more complex than over high purity aluminium specimens where the grain boundaries or cellular boundaries constitute only minor surface heterogeneities. Various alloying elements, introduced to improve mechanical strength, corrosion resistance, or to impart desirable colour shades after anodizing treatments, are present in the alloy as solid solutions, or forming second phases, such as zones, precipitates, or intermetallic compounds, of various shapes, sizes, and compositions (1). For better understanding of the porous film formation over microscopically heterogeneous aluminium alloy surfaces, precise knowledge is required of the highly localized processes, such as film formation, dissolution or both, proceeding over the second phases and their interplay with the general film formation over the surrounding matrix regions.

The purpose of the present paper is to show, through the study of porous film formation on an Al-1.4 wt % Fe alloy containing finely dispersed  $\text{Al}_6\text{Fe}$  and  $\text{Al}_3\text{Fe}$  particles, that the recent advances in energy-filtering transmission electron microscopy, allied with a novel specimen preparation technique of ultramicrotomy, provide an effective and important route towards the required understanding.

### 2. EXPERIMENTAL

An Al - 1.4 wt% Fe alloy, containing 0.02 % Si, 0.01 % Cu, and 0.01% Mg as major impurities, was prepared by Nippon Light Metal Company and supplied in the form of a 1 mm thick sheet with dimensions of 500 x 500 mm. The alloy was prepared by rapid solidification to allow the precipitation of finely dispersed  $\text{Al}_6\text{Fe}$  particles; however, the alloy also contains a small number of  $\text{Al}_3\text{Fe}$  particles. The alloy sheet was cut into strips of dimensions 10 mm x 50 mm. The strips were etched individually in 5 % NaOH solution at 25°C for 5 min, de-smutted in 50 %  $\text{HNO}_3$  at 25°C for 2 min, rinsed thoroughly in distilled water and, finally, dried in a warm air stream. Preliminary examination of the etched and subsequently de-smutted surfaces, by scanning electron microscopy, has revealed  $\text{Al}_6\text{Fe}$  particles of sizes up to about 3  $\mu\text{m}$  scattered over the scalloped surfaces. Most of the particles were of rod shape with aspect ratios up to around 1 : 10. Additionally,  $\text{Al}_3\text{Fe}$

particles of lath shape, up to several microns in size, were observed though only occasionally. The etched and de-smutted specimens were anodized in 2.4M  $\text{H}_2\text{SO}_4$  or 0.4M  $\text{H}_3\text{PO}_4$  solutions at 25°C and at a constant current density of 5 mA  $\text{cm}^{-2}$ .

Ultramicrotomed sections of the aluminium substrate and its porous film were prepared in the usual way using a RMC MT 6000 XL ultramicrotome (2). Briefly, the encapsulated specimens were trimmed initially with a glass knife, and suitably thin sections, about 10 nm thick, were prepared by sectioning in a direction approximately parallel to the oxide/metal interface using a diamond knife. The ultramicrotomed sections were examined generally in a JEM 2000 FXII transmission electron microscope operated at 200 kV. Selected specimens were examined further in a Philips CM 200/FEG/Ultra-twin transmission electron microscope equipped with a Gatan Imaging Filter (GIF); the microscope was operated at 200 kV.

### 3. RESULTS AND DISCUSSION

With successful preparation of cross-sectional specimens of the aluminium substrate and its porous film, through the ultramicrotomy approach, the morphologies and structures of the porous film developed around the  $\text{Al}_6\text{Fe}$  or  $\text{Al}_3\text{Fe}$  particles have been revealed with great precision, as shown in Fig.1-a and b. In both figures, the aluminium substrates are observed at the bottom of the micrographs. Above the aluminium substrates, porous films, about 0.4  $\mu\text{m}$  thick, are observed. Differences in the development of local film morphologies and structures around the  $\text{Al}_6\text{Fe}$  and  $\text{Al}_3\text{Fe}$  particles are immediately evident. In Fig.1-a, a dark  $\text{Al}_6\text{Fe}$  particle is observed within the porous film, apparently isolated from the metal. Further, the film/metal interface in such a region exhibits a ridged appearance and considerable branching of pores is observed beneath the entrapped  $\text{Al}_6\text{Fe}$  particle. In Fig.1-b, on the other hand, an  $\text{Al}_3\text{Fe}$  particle is observed near the film/metal interface, with the film/metal interface in the surrounding matrix regions and the film/ $\text{Al}_3\text{Fe}$  interface located at almost same depth from the film surface. In both cases, finely textured film materials are observed over the particles, as shown by the solid lines for clarity; such film materials represent porous oxide films grown by the oxidation of  $\text{Al}_6\text{Fe}$  or  $\text{Al}_3\text{Fe}$  particles and contain different amounts of iron (3).

It is readily understood that Figs. 1-a and b represent porous film formation over the local regions where the  $\text{Al}_6\text{Fe}$  or  $\text{Al}_3\text{Fe}$  particles were present at locations close to, but slightly beneath the initial etched surface. It is also readily understood that the shapes of the particles are represented approximately, though only cross sectional, by the areas defined by the solid lines. Through consideration of the development of these local features, the complex interplay between the local film formation over the  $\text{Al}_6\text{Fe}$  or  $\text{Al}_3\text{Fe}$  particles and general film formation over the surrounding matrix regions, as well as various factors involved, can be revealed and specified with great precision, as described briefly below.

During anodizing, porous film formation proceeds over the matrix surface above the particles in the usual manner and the film/metal interface recedes continuously inward. The receding film/metal interface eventually meets the  $\text{Al}_6\text{Fe}$  or  $\text{Al}_3\text{Fe}$  particles and the oxidation of the particles starts locally to form porous films containing iron, which exhibit finer textures than those grown over the matrix regions. Further development of local morphologies, structures, and compositions of the porous film in such regions depends on, among other things, the rates of porous film formation over the  $\text{Al}_6\text{Fe}$  or  $\text{Al}_3\text{Fe}$  particles, relative to that over the surrounding matrix regions. For the  $\text{Al}_6\text{Fe}$  case (Fig.1-a), porous film formation over the  $\text{Al}_6\text{Fe}$  particle proceeds at a rate of only about 40 % of that over the surrounding matrix regions (3). Thus, the film metal interface in the matrix regions around the particle recedes inward at a rate about twice as fast as that of the film/ $\text{Al}_6\text{Fe}$  interface. Further and at the faster receding film/metal interface around the  $\text{Al}_6\text{Fe}$  particle, pore branching starts to undercut aluminium beneath the particle which, depending on the shape and orientation of the particle, could lead to the incorporation of the particle before it had been oxidized completely. Under the present situation where a rod shaped  $\text{Al}_6\text{Fe}$  is present beneath the surface, with its long axis oriented approximately parallel to the initial etched surface, and where the rate of porous film growth over the particle is only about 40 % of that over the surrounding matrix regions, the particle becomes incorporated into the porous film grown over the surrounding matrix regions with about a third of its volume remaining unoxidized as observed in Fig.1-a.

Contrasting behaviour is observed for the  $\text{Al}_3\text{Fe}$  case where the rates of porous film growth over

the  $\text{Al}_3\text{Fe}$  particle and surrounding matrix regions are almost equal (3). In such a situation, the film/ $\text{Al}_3\text{Fe}$  interface and the film/metal interface in the surrounding matrix regions recede at almost equal rates. Accordingly, the  $\text{Al}_3\text{Fe}$  particles, whatever their shapes are, can never be incorporated into the porous film growing over the surrounding matrix regions. Thus, the only effect of the presence of the  $\text{Al}_3\text{Fe}$  particles is to give local regions where film composition and texture are different from those of the porous film grown over the surrounding matrix regions.

Through the examples given above, it is evident that the porous film formation over the microscopically heterogeneous aluminium alloy surfaces is very complex. Even in the relatively simple case where the second phase particles are oxidized, it is readily understood that the development of local morphologies, structures, and compositions of the film, associated with the presence of the second phase particles, are not determined by the rates of porous film growth over the particles alone, but also by the shapes and orientations of the particles.

In addition to the successful revelation of the complex interplay between the local film formation over the  $\text{Al}_6\text{Fe}$  and  $\text{Al}_3\text{Fe}$  particles and the general film formation over the surrounding matrix regions, close examination of the film/ $\text{Al}_6\text{Fe}$  or film/ $\text{Al}_3\text{Fe}$  interfaces by high resolution and energy-filtering transmission electron microscopy has revealed complex interfacial processes during the anodic oxide growth over the intermetallic particles which are of crucial importance for further understanding of the behaviour of intermetallic phases during anodizing of aluminium alloys generally.

Figure 2-a shows a so-called "direct or no-loss" image of the film/ $\text{Al}_3\text{Fe}$  interface. The image was obtained using electrons which suffered no-loss of energy and is essentially the same as the normal TEM image. Here, a dark band, a few nanometers in width, is observed clearly between the barrier layer of the porous film and the  $\text{Al}_6\text{Fe}$  particle. Additionally, the film/ $\text{Al}_6\text{Fe}$  interface exhibits a scalloped appearance of exceedingly fine dimensions, less than 10 nm.

Figure 2-b is essentially the same as Fig.2-a except that the image was obtained using electrons which underwent Fe-L loss. Thus, Fig.2-b effectively represents an iron-distribution map of the area examined; the high local density of white-dots in the micrograph, corresponds to regions with the high local concentration of iron. Here, the Fe-L loss image was acquired and processed using 3 - interval background extrapolation and subtraction. Processing time per 512 x 512 pixel map was less than 30 s. It is evident that iron is distributed uniformly within the  $\text{Al}_6\text{Fe}$  particle, as well as in the porous oxide grown over the particle, as expected. Additionally and importantly, it is clearly demonstrated that the dark band observed between the barrier layer of the porous film and the  $\text{Al}_6\text{Fe}$  particle represents a narrow region of iron enrichment.

For the films formed in a sulphuric acid solution where the film/ $\text{Al}_6\text{Fe}$  interface exhibits a scalloped geometry of exceedingly fine dimensions, less than 10 nm, which is comparable to the thickness of ultramicrotomed section prepared, sole structural examination of the iron enriched layer was not possible due to overlapping of two or three pores in the region examined. To overcome this difficulty, the alloy was anodized in 0.4M  $\text{H}_3\text{PO}_4$  solution to obtain a relatively large featured porous film so that the iron enriched layer is observed in ultramicrotomed sections as a single discrete layer with a sharply defined film/ $\text{Al}_6\text{Fe}$  interface. Examination of such film/ $\text{Al}_6\text{Fe}$  interfaces in a Philips CM200/FEG/Ultra-twin transmission electron microscope with a point-to-point resolution better than 0.19 nm has revealed successfully structural details of the iron enriched layer at atomic scale resolution (4). It was found that the iron enriched layer, about 1 nm in width, has a heavily distorted structure with occasional presence of ordered domains, only 1 nm diameter, with the  $\text{Al}_6\text{Fe}$  structure. No evidence was obtained, however, to suggest the presence of iron sub-nano or nano-clusters in the enriched layer. EDX analysis of the enriched layer using an focused electron probe of diameter of about 1 nm has shown that the composition of the enriched layer may be represented approximately by  $\text{Al}_{80}\text{Fe}_{20}$ , confirming significant enrichment of iron in the narrow region. Thus, it has been demonstrated, for the first time, that the anodic oxide formation on the  $\text{Al}_6\text{Fe}$  intermetallic phase involves initial and selective oxidation of aluminium and interfacial enrichment of iron, with the enrichment confined into a thin layer, about 1 nm thick, in the  $\text{Al}_6\text{Fe}$  phase immediately beneath the oxide film. The formation of the iron enriched layer can be explained reasonably in the frame of the Gibbs free energy criteria for alloy oxidation presented recently by five of the present authors (5).

In conclusion, the present work demonstrates clearly that the combined use of energy-filtering transmission electron microscopy and ultramicrotomy is able to provide morphological, structural and compositional details of local regions of interest with atomic scale resolution and with direct and one-to-one correspondence to the microscopical surface heterogeneities. Therefore the present approach is expected to play a greater role in the future studies of corrosion and filming behaviour of aluminium alloys of practical importance over many years to come.

#### **ACKNOWLEDGEMENTS**

The authors wish to acknowledge the Light Metal Educational Foundation, Osaka, Japan for support of this work. One of the authors(G.M.B.) wishes to gratefully acknowledge the support of Japan Society for Promotion Science(JSPS) post-doctoral fellowship.

#### **REFERENCES**

- [1] L.F.Mondorfo, in "Aluminium alloys", Butterworth, London 1976
- [2] R.C.Furneaux, G.E.Thompson, and G.C.Wood, Corros.Sci. 18, 853 (1978).
- [3] K.Shimizu, G.M.Brown, K.Kobayashi, P.Skeldon, G.E.Thompson, and G.C.Wood, ATB Metallurgy, 37, No.2-3-4, 188 (1997).
- [4] K.Shimizu, G.M.Brown, H.Habazaki, K.Kobayashi, P.Skeldon, G.E.Thompson, and G.C.Wood Corros.Sci. in press.
- [5] H.Habazaki, K.Shimizu, P.Skeldon, G.E.Thompson, G.C.Wood, and X.Zhou, Trans.Inst.Met.Finish. 75, 18 (1997).



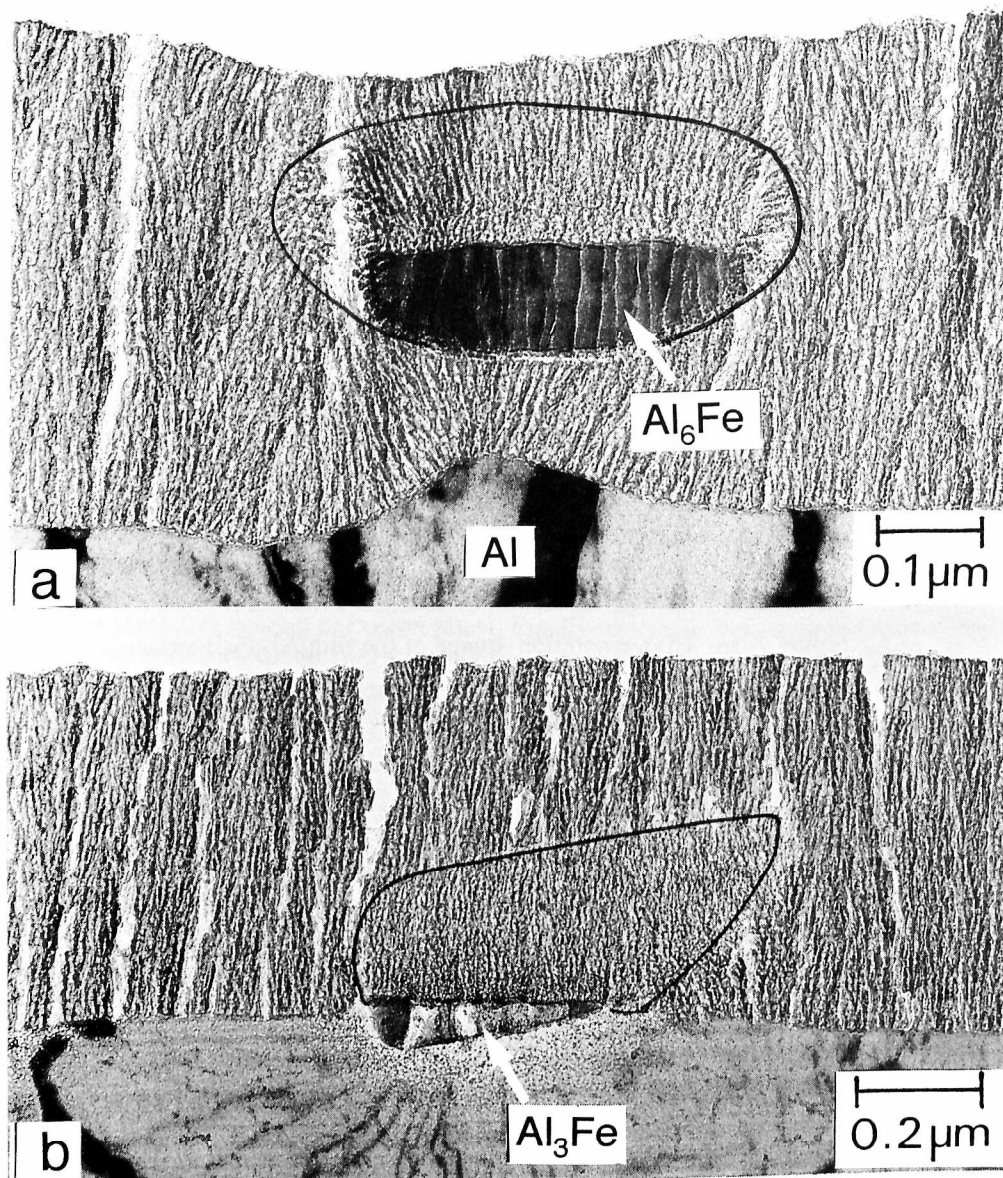


Figure 1 Transmission electron micrographs of ultramicrotomed sections of the aluminium substrate and its porous film, showing local film formation over the regions where (a)  $\text{Al}_6\text{Fe}$  and (b)  $\text{Al}_3\text{Fe}$  particles were present beneath the initial etched surface.

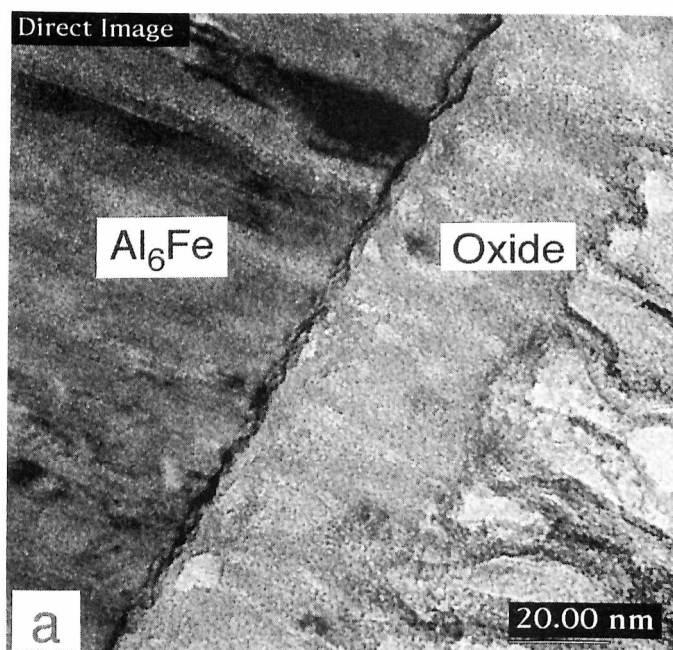


Figure 2- (a) High resolution image of the film/ $\text{Al}_6\text{Fe}$  interface

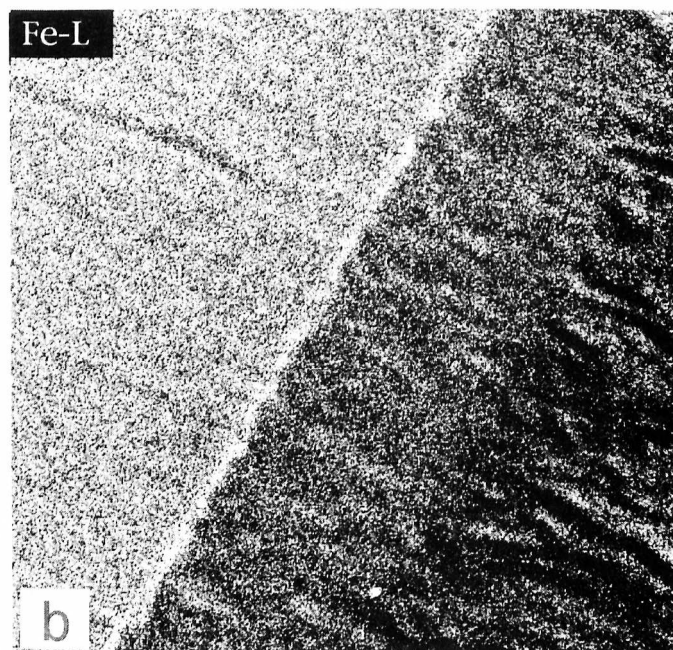


Figure 2- (b) As (a) but, Fe-L loss image, showing iron enrichment at the film/ $\text{Al}_6\text{Fe}$  interface.